



HAL
open science

Different secretory repertoires control the biomineralization processes of prism and nacre deposition of the pearl oyster shell.

Benjamin Marie, Caroline Joubert, Alexandre Tayalé, Isabelle Zanella-Cléon, Corinne Belliard, David Piquemal, Nathalie Cochenec-Laureau, Frédéric Marin, Yannick Gueguen, Caroline Montagnani

► To cite this version:

Benjamin Marie, Caroline Joubert, Alexandre Tayalé, Isabelle Zanella-Cléon, Corinne Belliard, et al.. Different secretory repertoires control the biomineralization processes of prism and nacre deposition of the pearl oyster shell.. Proceedings of the National Academy of Sciences of the United States of America, 2012, 109 (51), pp.20986-20991. 10.1073/pnas.1210552109 . hal-00786507

HAL Id: hal-00786507

<https://hal.science/hal-00786507>

Submitted on 29 May 2020

HAL is a multi-disciplinary open access archive for the deposit and dissemination of scientific research documents, whether they are published or not. The documents may come from teaching and research institutions in France or abroad, or from public or private research centers.

L'archive ouverte pluridisciplinaire **HAL**, est destinée au dépôt et à la diffusion de documents scientifiques de niveau recherche, publiés ou non, émanant des établissements d'enseignement et de recherche français ou étrangers, des laboratoires publics ou privés.

Different secretory repertoires control the biomineralization processes of prism and nacre deposition of the pearl oyster shell

Benjamin Marie^{a,b,1,2}, Caroline Joubert^a, Alexandre Tayalé^a, Isabelle Zanella-Cléon^c, Corinne Belliard^a, David Piquemal^d, Nathalie Cochennec-Laureau^{a,e}, Frédéric Marin^b, Yannick Gueguen^a, and Caroline Montagnani^{a,f,2}

^aIfremer, Centre Ifremer du Pacifique, Unité Mixte de Recherche 241 Ecosystèmes Insulaires Océaniques, Tahiti, 98719 Taravao, French Polynesia; ^bUnité Mixte de Recherche 6282 Centre National de la Recherche Scientifique, Biogéosciences, Université de Bourgogne, 21000 Dijon, France; ^cCentre Commun de Microanalyse des Protéines, Unité Mixte de Service 344/Unité de Service 8 BioSciences Gerland-Lyon Sud, Institut de Biologie et de Chimie des Protéines, 69007 Lyon, France; ^dSkuldtech, 34184 Montpellier, France; ^eIfremer, Station de la Trinité-sur-mer, 56470 La Trinité-sur-mer, France; and ^fIfremer, Unité Mixte de Recherche 5119 ECOLOGIE des SYstèmes Marins Côtiers, Université Montpellier II, 34095 Montpellier, France

Edited* by Andrew H. Knoll, Harvard University, Cambridge, MA, and approved October 31, 2012 (received for review July 9, 2012)

Mollusca evolutionary success can be attributed partly to their efficiency to sustain and protect their soft body with an external biomineralized structure, the shell. Current knowledge of the protein set responsible for the formation of the shell microstructural polymorphism and unique properties remains largely patchy. In *Pinctada margaritifera* and *Pinctada maxima*, we identified 80 shell matrix proteins, among which 66 are entirely unique. This is the only description of the whole “biomineralization toolkit” of the matrices that, at least in part, is thought to regulate the formation of the prismatic and nacreous shell layers in the pearl oysters. We unambiguously demonstrate that prisms and nacre are assembled from very different protein repertoires. This suggests that these layers do not derive from each other.

mantle | mollusk shell matrix proteins | proteome | transcriptome | evolution

A wide variety of organisms synthesize biomineralized structures used for maintaining their soft bodies, protecting them from predators, perceiving the magnetic field or gravity, or storing inorganic ions (1). The ability to construct a mineralized exoskeleton is thought to be one of the key factors that triggered the expansion of metazoan life at the dawn of the Cambrian times. Our understanding of the evolutionary pattern of mineralizing metazoans is intimately linked to the comprehension of the way in which metazoans acquired the capacity to construct mineralized body part. The genes and molecular mechanisms that control biomineralization processes are gradually being identified (2, 3). In addition to their mineral moieties, metazoan skeletons—in particular those constructed from calcium carbonate—contain an organic extracellular matrix. During mineralization processes, this secreted matrix potentially interacts with the mineral phase. According to the most commonly accepted views, the matrix is thought to regulate different aspects of crystal deposition: initiation of mineralization, assembly in mesocrystalline structures, and inhibition (4–6). Thus, this matrix, which remains occluded within the mineral phase once formed, plays a central role in the entire biomineralization process.

For over 500 million years, mollusks have successfully used a wide variety of shells to populate the world (7). The mollusk shell is constructed of different calcium carbonate layers, which are precisely assembled in defined microstructures, such as prisms, nacre, foliated, or crossed-lamellar. Most of these textures appeared in the Early Phanerozoic, suggesting that mollusks rapidly explored a large set of combinations of microstructures to elaborate their shell (8–10). Since their emergence, these shell microstructures have proven to be remarkably stable and perennial from a morphological viewpoint. Among the most studied of them are the nacre-prismatic shells of Cambrian origin (9). Such a composite material combines the respective mechanical properties of each layer. The calcitic outer layer often presents high crack propagation and puncture-resistance properties, and the nacreous internal layer

is characterized by an extremely high fracture resistance, accompanied by a higher ductility. Hence, the external layer rather constitutes a primary barrier, whereas nacre dissipates energy and stops cracks (11–13). Complex environmental selection pressures (biotic, abiotic) may have favored the appearance and maintenance of such structures (14, 15). However, the origin of both prisms and nacre remains enigmatic (16, 17). Even more elusive are the molecular processes involved in prisms and nacre deposition and the identification of the “molecular toolkit” required for the emergence of these microstructures from liquid/colloidal precursors.

To identify the proteinaceous “actors” that contribute to generate prisms and nacre, we performed a high-throughput comparison of the occluded shell protein repertoire—at transcript and protein levels—expressed during the deposition of these two calcified layers in the Polynesian pearl oyster *Pinctada margaritifera*. Our data provide strong evidence that the proteinaceous matrices associated with prism and nacre are extremely different. This observation was confirmed by parallel analysis performed on a closely related species, the gold-lip oyster *Pinctada maxima*. Our results highlight our understanding of the molecular mechanism of prism and nacre formation and have major implications for the evolutionary scenarios of the origin of these two shell microstructures, arguing against the matrix proteins of one layer being the precursor of those in the other.

Results

Organic Shell-Layer Matrices. The shell of *Pinctada* sp. exhibits a trilayered structure composed of a thin organic external layer, the periostracum, and two calcified layers: an outer prismatic calcitic and an inner nacreous aragonitic layer (18). The nacre consists of a laminar structure composed of 0.5- μ m thick polygonal flat tablets surrounded by a thin organic matrix, organized in a brick wall-like structure (Fig. 1A). Prisms are calcitic needles of much bigger size, packed in an organic sheath. They grow

Author contributions: B.M., N.C.-L., F.M., Y.G., and C.M. designed research; B.M., C.J., A.T., I.Z.-C., C.B., and C.M. performed research; C.J. and A.T. contributed new reagents/analytic tools; B.M., C.J., A.T., I.Z.-C., D.P., F.M., and C.M. analyzed data; and B.M., C.J., F.M., Y.G., and C.M. wrote the paper.

The authors declare no conflict of interest.

*This Direct Submission article had a prearranged editor.

Data deposition: The sequences reported in this paper have been deposited in the GenBank database [accession nos. HE610373–HE610410 (*P. margaritifera* CDs)] and in the Swiss-Prot database [accession nos. P86947–P86969 (*P. maxima* proteins) and H2A0K6–H2A0P3 (*P. margaritifera* proteins)].

¹Present address: Unité Mixte de Recherche 7245 Centre National de la Recherche Scientifique Molécules de Communication et Adaptation des Micro-organismes, Muséum National d'Histoire Naturelle, 75005 Paris, France.

²To whom correspondence may be addressed. E-mail: bmarie@mnhn.fr or caroline.montagnani@ifremer.fr.

This article contains supporting information online at www.pnas.org/lookup/suppl/doi:10.1073/pnas.1210552109/-DCSupplemental.

perpendicularly to the external shell surface (Fig. 1B). Here, we analyzed the acid-insoluble matrices (AIMs) associated with these two microstructures because both prism or nacre AIMs represent more than 90% of the total shell matrices. The AIMs of both prism and nacre layers are mainly proteinaceous. A bulk amino acid analysis indicates high amounts of Gly residues (30%; Fig. S1A and B), but both AIMs have a slightly different amino acid signature: Prism AIM is enriched in Tyr, Pro, and Val, and nacre AIM in Ala and Asx residues. Both AIMs can be partly solubilized in a denaturing solution (Laemmli-solubilized fraction). When run on SDS/PAGE and stained with Coomassie brilliant blue, the prism and nacre AIMs revealed various distinct proteinaceous bands (Fig. S1C) that were further investigated by mass spectrometry for protein identification.

Protein Composition of Shell-Layer Matrices. We analyzed the unfractionated prism and nacre AIMs of *P. margaritifera* and, in parallel, the bands obtained from SDS/PAGE by proteomics (Fig. S1C). We identified 78 different shell matrix proteins (SMPs), among which 64 are entirely unique. Among the proteins described here are nacre uncharacterized shell protein 1 (NUSP-1), Clp-1, Clp-3,

epidermal growth factor 1 (EGF-1), EGF-2, Cement-like, Alveolin-like, or MP10 (Fig. S2). From the whole set, 45 are exclusive to prisms, and 30 to nacre. Only three proteins are detected in both layers (Figs. 1C and D and 2; Datasets S1 and S2).

To confirm *P. margaritifera* protein identification, we applied a similar proteomic approach to the calcified shell layers of *P. maxima*, a closely related species (19, 20). Fig. 1 presents the list of *P. margaritifera* identified proteins that exhibit at least two matching peptides or that have been further identified in *P. maxima*. Fig. 2 synthesizes the information on the protein content in the two shell layers, in the two *Pinctada* species (Datasets S1 and S2). From the 78 SMPs detected in *P. margaritifera* nacre and prisms, 41 “homologous” ones are detected in *P. maxima*, from a total of 43 SMPs in this latter species. Although bias is possible, we show that (i) we have obtained most of the main SMPs that are required for fabricating a shell; (ii) the shell secretory repertoires of prisms and nacre are truly different in both *Pinctada* species (Figs. 1 and 2; Datasets S1 and S2). Except for Nacrein, Shematrin-8, and NUSP-18, all of the 77 other *Pinctada* SMPs appear to be exclusively detected in only one of the two shell layers (Fig. 2).

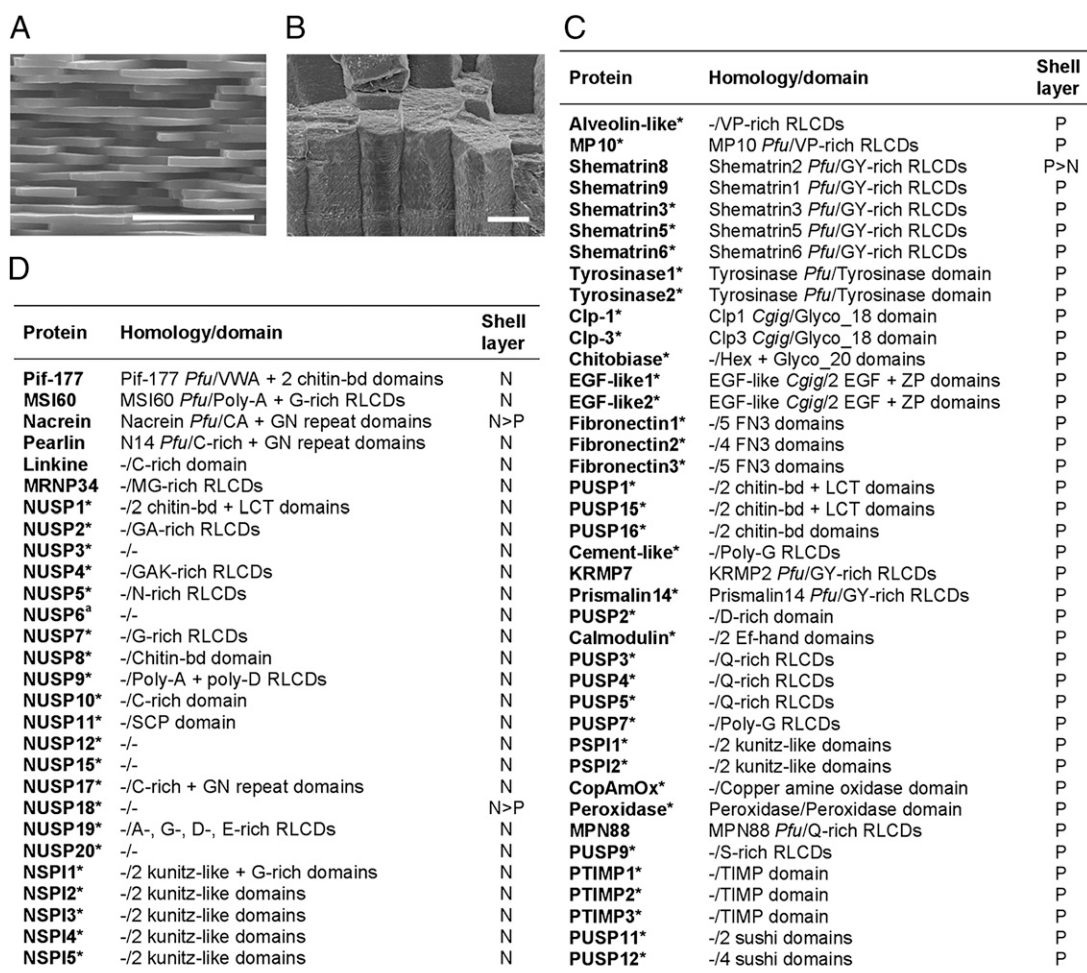


Fig. 1. *P. margaritifera* prism and nacre SMPs. The nacre (A) and prism (B) AIM proteins were digested with trypsin, and the resulting peptides were analyzed by mass spectrometry (MS/MS mode). *P. margaritifera* prism (C) and nacre (D) SMPs that presented at least two matching peptides, or for which identification was further confirmed in *P. maxima* by homolog protein detection, are listed. Raw MS/MS data were directly interrogated against the assembled mantle EST data set (17). An asterisk indicates protein sequences discovered in this analysis. Predicted signal peptide can be retrieved from all EST-translated products that match shell proteomic data, indicating that these proteins are secreted. Full-length sequences of 52 unique SMPs (17 nacre and 35 prism proteins) were deposited on National Center for Biotechnology Information database (Datasets S1 and S2). No additional proteins were identified from the *P. margaritifera* prism and nacre acid-soluble matrices (Table S1). N: nacre; P: prism; *Pfu*: *Pinctada fucata*; *Cgig*: *Crassostrea gigas*. “>” indicates that mass spectrometry identification scores are higher in one of the two layers when detected in both shell AIMs. Shematrin8 was then considered as prism SMP, and Nacrein and NUSP-18 as nacre SMPs, accordingly. (Scale bars, 5 and 50 μ m for A and B, respectively.)

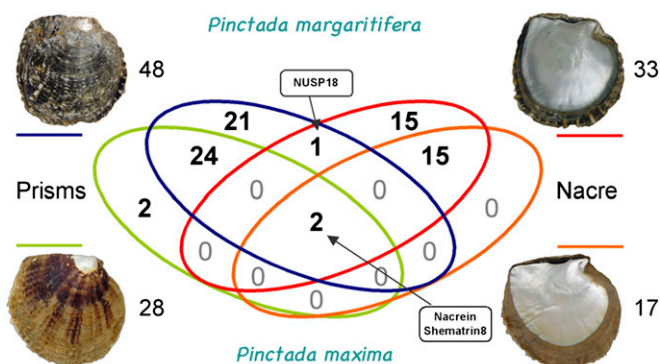


Fig. 2. Comparison of prism and nacre SMPs of *P. margaritifera* and *P. maxima*. Prisms and nacre proteins identified in both species by MS/MS analyses are circled in blue/green or red/orange, respectively. In *P. margaritifera*, 48 proteins were detected in prisms, and 33 in nacre. Forty-five proteins are prism-specific and 30 are nacre-specific. Only three proteins are common to the two layers. In *P. maxima*, 28 proteins were detected in prisms (with 26 prism-specific), 17 in nacre (with 15 nacre-specific), and only 2 in common proteins. Twenty-four proteins are common to *P. margaritifera* and *P. maxima* prism AIMS, and 15 are common to both nacres. From the 43 SMPs detected in *P. maxima*, 41 homologs can be retrieved in *P. margaritifera* and present high sequence similarities (above 85–95% sequence identity), giving a congruent picture with previous phylogenetic data for these species (20). From the 80 different *Pinctada* SMPs identified here, 77 can be specifically detected in prisms and nacre. Three proteins only, Sshmatrin8, Nacrein, and NUSP-18, are found in both shell layers.

Immunolocalization of Proteins from *P. margaritifera* Nacre. We developed specific polyclonal antibodies raised against the Laemmli-solubilized proteins of the nacre AIM fraction of *P. margaritifera*. Interestingly, these antibodies, which react with a large set of nacre SMPs, do not exhibit cross-reactivity with the prism matrix when analyzed on Western blot (Fig. 3A). This suggests that the main immunogenic epitopes of nacre SMPs are not present in the prism SMPs. The immunogold observations of nacre cross-sections revealed that the nacre antibodies exhibit a very clear and specific signal on nacre, mostly localized in the interlamellar matrix that separates nacre layers (Fig. 3B). Furthermore, the nacre protein localization within the mantle epithelium clearly revealed that they are exclusively synthesized in the dorsal zone (mantle pallium), which is supposedly responsible for nacre deposition (21), and not in the ventral zone, which is involved in the prismatic layer formation (Fig. 3C).

SMP Gene Expression Patterns. Quantification of SMP gene transcripts in oyster tissues. To test the specificity of a large set of SMP gene expression, we performed high-throughput quantitative RT-PCR (qRT-PCR) analyses on mantle edge and pallium and other tissues of *P. margaritifera*. We analyzed the expression pattern of 61 selected genes encoding 38 and 23 SMPs from the prismatic and the nacreous layers, respectively (primer list and all quantitative PCR data are in [Datasets S1–S3](#)). Strikingly, all SMP-encoding genes present a very clear and specific strong expression in mantle tissues in comparison with muscle, gills, digestive gland, gonads, and hemocytes (Fig. S3). Moreover, the comparison of mantle edge and pallium expression of SMP genes clearly revealed that all prism-specific SMP gene expression levels are higher in mantle edges, whereas all nacre-specific SMP gene expressions are more intensive in mantle pallium (Fig. 4). These results show that the calcifying genes are specifically expressed in the mineralizing tissues and can be discriminated on the basis of their respective expression site, i.e., the mantle edge for “prism-related genes” and the mantle pallium for “nacre-related genes.”

Localization of SMP gene transcripts in oyster tissues. We further investigated the mantle expression pattern of six proteins, three of which are specifically implicated in the biomineralization of the prisms (MP10, Clp-1, and Fibronectin-1) and the three others (NUSP-1, Pearlin, and MRNP34) in that of nacre. In situ hybridization (ISH) analyses revealed that all these transcripts were specifically restricted to the monolayered cells of the outer calcifying mantle epithelium (Fig. 5). More specifically, these transcripts were localized in two distinct areas: the mantle edge for MP10, Clp-1, and Fibronectin-1 and the mantle pallium for NUSP-1, Pearlin, and MRNP34. The expression of the prism protein genes abruptly stops at one unique cellular limit beyond which the expression of genes that encode nacre protein starts. We also observed that the expression pattern of some genes may be more nuanced: MRNP34 exhibits a gradually increasing expression pattern within the transition zone from the prisms to the nacre. We assume that the slight distinction between ISH and qRT-PCR results (strong zonation versus more contrasted expression) is mainly due to technical sensitivity differences.

Discussion

Distinct Prism Versus Nacre Protein Assemblages. We have developed a combined proteomic/transcriptomic approach to identify the whole assortment of proteins associated with the prisms and nacre layers in pearl oyster shells. This represents a comprehensive characterization of proteins associated with different shell microstructures among mollusks. Our findings provisionally

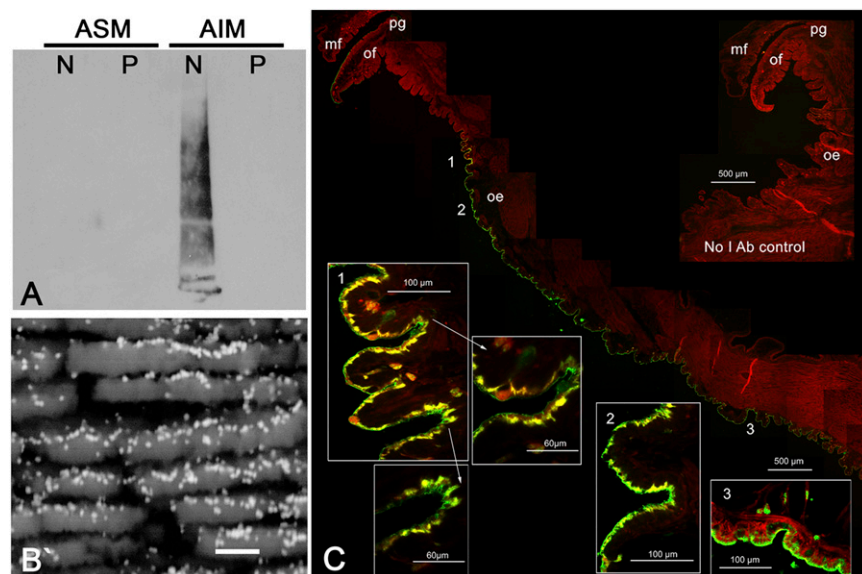


Fig. 3. Immunolocalization of nacre SMPs on shell and mantle of *P. margaritifera*. A polyclonal antibody raised against a solubilized fraction of nacre AIM was used to identify nacre proteins (A) on Western blot (N, nacre; P, prisms), (B) in nacre cross-section by immunogold (scale bar, 1 μ m), and (C) in mantle epithelia by immunofluorescence. mf: middle fold; of: outer fold; pg: periostacal groove; oe: outer epithelium. We note that the fact that more gold particles are observed on the upper interlamellar side of nacre tablets, rather than on the down side, is mainly due to the microtopography of nacre fractures and to the angle of observation.

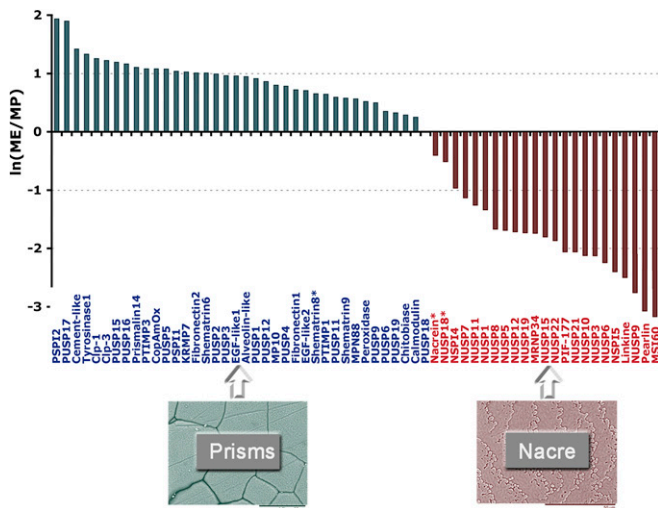


Fig. 4. Prism and nacre SMP gene expression in mantle edge and pallium of *P. margaritifera* estimated by high-throughput qRT-PCR (Fluidigm). Comparison of $\ln(\text{ME}/\text{MP})$ expression ratio (fold/fold) of prism and nacre SMPs. Protein names are indicated in blue and red colors for prism and nacre SMPs, respectively. The three SMPs detected in both prism and nacre layers are indicated with an asterisk.

close the debate on the “prism/nacre” question. Is the deposition of these two microstructures regulated by similar or by different sets of macromolecules?

This puzzling issue (22) was initially debated more than a century ago, when Wetzel (23) compared the amino acid composition of bulk matrices associated with prisms and nacre and observed differences in both layers, a finding that was later confirmed by Hare (24). A chromatographical approach allowed Weiner (25, page 4144) to “decorticate” more precisely the soluble prism and nacre matrices of the California mussel. The tenets of his results were that “approximately half [of the] matrix constituents are common to both layers and half, specific to one of the layers.” Thirteen years, however, were required before the release of the full-length SMP sequence Nacrein (26) and the further identification of this protein in both layers (27). Since then, several new proteins have been retrieved by a “one-per-one” approach. However, this strategy did not give any chance to obtain the full picture of the protein repertoire, and, to date, only 14

SMPs have been described in *Pinctada* sp. from nacre and prisms (28, 29). On the other hand, approaches at the transcript level performed during these past years have shown that some of these shell proteins, together with other secreted or nonsecreted proteins, exhibited a delimited spatial gene expression in the outer mineralizing mantle-epithelial cells of the pearl oyster (30, 31) or of the ormer (32).

We have identified 80 different *Pinctada* SMPs, among which 66 are entirely unique. By dramatically increasing the number of identified SMPs, the present work sheds a light on the molecular diversity of bivalve calcifying matrices and on the potential function of these SMPs in the specific mechanisms of prism and nacre biomineralization (33). Further characterizations of the structural interaction between this set of SMPs, the chitin framework, and calcium carbonate polymorphs should help us to refine the models of matrix framework organization and control in shell formation processes (Fig. S5). Although our data support the idea of a SMP control of the microstructure deposition (34), all of the biomineral-associated compounds are not necessarily involved in the formation of the calcium carbonate polymorphs (calcite versus aragonite) and of the specific microstructures (prisms versus nacre). The question about how and which one of these macromolecules specifically regulates these processes thus remains an open one.

In *Pinctada* sp. we described 47 proteins that are exclusive to prisms (from a total of 50 prism-associated SMPs) and 30 proteins exclusive to nacre (from a total of 33 nacre-associated SMPs). From the 61 SMP-encoding transcripts whose expression pattern was investigated, a very large majority exhibited exclusive overexpression in mantle edge or mantle pallium cells in concordance with the presence of their translated product either in prism or in nacre. Combining the proteomic, transcriptomic, and immunological approaches, we demonstrate unambiguously that the molecular toolkits, i.e., protein assortments, secreted by the mantle edge, and the mantle pallium, incorporated within the biomineral phase and potentially responsible for the deposition of prisms and nacre, respectively, are extremely different.

Diversity of SMP Domains. Our finding at the protein level is also true at the protein domain level. With few exceptions, most of the protein domains associated with each layer are different and exhibit distinct signatures. On one side, the prism protein domains are characterized by the occurrence of numerous characteristic extracellular matrix (ECM) domains, comprising EGF-like, zona pellucida, fibronectin-3, EF-hand, sushi, and tissue inhibitor of metalloproteinase. On the other side, the known ECM domains of nacre proteins are limited to von Willebrand A and secreted

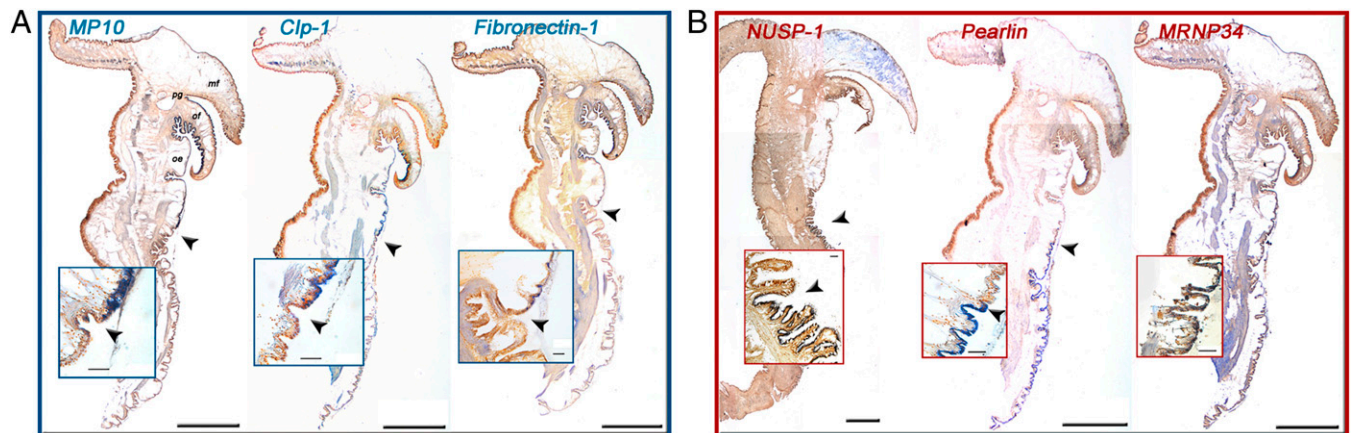


Fig. 5. Localization of prism and nacre transcripts in *P. margaritifera* mantle by in situ hybridization. (A) MP10, Clp-1, and Fibronectin-1 transcripts are expressed in the outer epithelium of the mantle edge. (B) NUSP-1, Pearlin, and MRNP34 transcripts are expressed in the outer epithelium of the mantle pallium. Paraffin-embedded sections of oyster tissues were hybridized with antisense or sense single-stranded cDNA probes labeled with digoxigenin. Positive cells are stained in dark blue. Sense probes showed no hybridization (Fig. S4). Black arrows symbolize the epithelial cell limits of prism and nacre transcript expression. (Scale bars, 1 mm in large view and 50 μm on stained-cell enlargements.) mf: middle fold; of: outer fold; pg: periostracal groove; oe: outer epithelium.

cysteine-rich protein. In addition, the prism matrix is characterized by the presence of two types of chitinases (glyco_18 and glyco_20), copper amine oxidases, peroxidases, and tyrosinases, which are absent from the nacre matrix proteins. Repeated low complexity domains (RLCDs) are another point in case: they are frequent in proteins associated with calcified tissues (35). Here, we observe that RLCDs are different in prisms and nacre proteins. Those from prism proteins are of the Q-rich, S-rich, V-rich, and GY-rich types, whereas those from nacre proteins are A-rich, C-rich, D-rich, GA-rich, GN-rich, and MG-rich (Fig. 1; [Datasets S1 and S2](#)). We also observed that few prism and nacre proteins that are truly different exhibit domains with similar signatures. These domains are of three kinds: chitin-binding, lectin, and Kunitz-like. These shared domains emphasize that both prism and nacre matrices (i) contain chitin and other polysaccharides (33, 36, 37) and (ii) require a self-protecting system that precludes extracellular proteolysis (38, 39). However, these functional similarities are marginal and do not attenuate our main findings, i.e., the unrevealed diversity of SMP domains and the fundamental difference between the protein repertoires associated with prisms and nacre.

Origin of Prisms and Nacre. As described in earlier works (9, 40), the combination of prism–nacre microstructures in mollusk shells represents, from an evolutionary viewpoint, a successful innovation that was acquired somewhere in the Cambrian, among different mollusk lineages, in particular bivalves. This innovation was seemingly conserved in many taxa and kept morphologically unchanged since then, despite the high energy cost required for its synthesis in comparison with other shell microstructures (41).

What is the origin of the diverse shell microstructures in mollusks? Ontological and paleontological data give congruent pictures. On one hand, the ontogenic data obtained on the modern pearl oysters (42, 43) or other pteriomorphid bivalves (44) indicate that the first shell produced is organic (periostracum-like); this shell is then mineralized and made of aragonite granules (prodissoconch I). This step precedes the deposition of calcitic prisms (prodissoconch II), followed by the deposition of the nacreous layer after metamorphosis. On the other hand, from a paleontological viewpoint, *Pojetaia runnegari*, usually considered to be one of the earliest bivalves of the Lower to Middle Cambrian and the ancestor of nacro-prismatic nuculidae, seems to have exhibited a single-layer shell made of a prism-like biomineral deposited on a periostracal layer (8). This event occurred not too long before the appearance of the association of prisms and nacre, which may be arguably considered among the most primitive microstructure combinations in adult mollusk shells (8, 45). How multilayered shell emerged is not known, but few attempts to establish a filiation between different shell microstructures have been initiated. In particular, Taylor et al. (40) suggested that different shell microstructures might have derived from one ancestral type through the reorganization of the shell crystallites. Carter and Clark (46, page 67) proposed that “nacre evolved through simple horizontal partitioning of vertical prisms.” This interesting viewpoint gives a mechanistic explanation for describing the genesis of nacre from prisms (Fig. S6), but is not corroborated by experimental evidences. Our molecular data on prisms and nacre protein sets do not support a direct filiation between these two microstructures, but rather suggest that their assembling is performed from two molecular toolkits that do not derive one from the

other. If nacre appeared after prisms, this event should be considered as a true evolutionary innovation, and not as the result of a duplication and subsequent structural rearrangement of the prismatic layer.

Physiological, Cellular, and Regulatory Aspects of Shell Mineralization. Observations of shell structure indicate a marked interruption of the mineral deposition within the transitory area between prisms and nacre (18). Indeed, the first transitional aragonite crystals that precede and support the deposition of the first nacre tablets appear to be always nucleated on the peri-prismatic organic membrane and never directly on prism crystallite itself (Fig. S7). In addition to our protein composition analysis, elemental mapping revealed that elemental composition of prism and nacre layers is also different with regard to Mg, Na, S, or Cl contents (47). Taken together, these data do not support the existence of a continuous extrapallial fluid filling the empty space between the mantle epithelium and the shell (48), but rather argue for an intimate contact between the mantle cells and the growing shell surface (49).

The mantle edge is considered to be responsible for the formation of the periostracum and of the prismatic layer, whereas the mantle pallium enables the formation of the nacreous layer (21, 30, 50). Our molecular observations fully confirm this spatial dichotomy and call for emerging questions on the regulation of shell mineralization by mantle epithelium. This molecular dissimilarity is corroborated by recent ultrastructural investigation of the mantle epithelia (51), suggesting cellular differentiation of prisms and nacre-secreting cells. However, a true cell secretion plasticity is maintained: experiments on shell repair (52) or on the formation of grafted pearls (53) show that the mantle epithelial or pearl sac cells can transiently change the mineralogy and the microstructure of the deposited layer, very likely according to a drastic change in the matrix secretory regime. The molecular regulatory mechanisms upstream from the secretory cascade remain unknown (54). They should, however, constitute an important focus for future research that explores the cellular and molecular basis of shell formation.

Materials and Methods

The extraction of shell matrices and immunogold localization were performed in Dijon, France. Proteomic analyses were performed at the Institut de Biologie et de Chimie de Protéines (Lyon, France). Transcriptomic and tissue immunolocalization analyses were performed at the Centre Ifremer du Pacifique (French Polynesia) and at the Génomol (Toulouse, France). Computational analyses were performed at Skuldtech (Montpellier, France). All analyses are detailed in [SI Materials and Methods](#).

ACKNOWLEDGMENTS. We thank Dr. Marcel Le Pennec, Dr. Denis Saulnier, Mr. Péva Levy, Dr. Cédrik Lo, Mrs. Anne-Sandrine Talfer, and Mrs. Nathalie Guichard for helpful discussions and assistance. The authors thank the two anonymous reviewers for their valuable and constructive comments on the first version of the manuscript, which helped improve the quality of the paper. This study is part of a collaborative project (Groupe De Recherche ADEQUA) supported by the “Direction des Ressources Marines” of French Polynesia. It is also supported by Ifremer, the University of French Polynesia, and the University of Burgundy. The work of F.M. was supported by Agence Nationale de la Recherche funding (ACCRO-EARTH, ref. BLAN06-2_159971, Gilles Ramstein, Laboratoire des Sciences du Climat et de l’Environnement) during the period 2007–2011 and by the COST (European Cooperation in Science and Technology) project TD0903 (Biomineralex; [www.biomineralex.eu](#); 2009–2013).

1. Lowenstam AH, Weiner S (1989) *On Biomineralization* (Oxford Univ Press, New York).
2. Kawasaki K, Suzuki T, Weiss KM (2004) Genetic basis for the evolution of vertebrate mineralized tissue. *Proc Natl Acad Sci USA* 101(31):11356–11361.
3. Killian CE, Wilt FH (2008) Molecular aspects of biomineralization of the echinoderm endoskeleton. *Chem Rev* 108(11):4463–4474.
4. Mann S (1988) Molecular recognition in biomineralization. *Nature* 332:119–124.
5. Falini G, Albeck S, Weiner S, Addadi L (1996) Control of aragonite or calcite polymorphism by mollusk shell macromolecules. *Science* 271:67–69.
6. Weiner S, Addadi L (1997) Design strategies in mineralized biological materials. *J Mater Chem* 7:689–702.
7. Ponder WF, Lindberg DR (2008) *Phylogeny and Evolution of the Mollusca* (Univ of California Press, Berkeley).
8. Runnegar B (1985) Shell microstructures of Cambrian mollusc replicated by phosphate. *Alcheringa* 9:245–257.
9. Kouchinsky A (2000) Shell microstructures in Early Cambrian molluscs. *Acta Palaeontol Pol* 45(2):119–150.
10. Feng W, Sun W (2003) Phosphate replicated and replaced microstructure of molluscan shells from the earliest Cambrian of China. *Acta Paleontol Pol*. 48:21–30.
11. Jackson AP, Vincent JFV, Turner RM (1988) The mechanical design of nacre. *Proc R Soc Lond B Biol Sci* 234:415–440.

12. Taylor J, Layman M (1972) The mechanical properties of bivalve (Mollusca) shell structures. *Paleontology* 15(Pt 1):73–87.
13. Li X, Chang W-C, Yuh JC, Wang R, Chang M (2004) Nanoscale structural and mechanical characterization of a natural nanocomposite material: The shell of red abalone. *Nano Lett* 4:613–617.
14. Harper EM (2000) Are calcitic layers an effective adaptation against shell dissolution in the Bivalvia? *J Zool (Lond)* 251:176–186.
15. Porter SM (2007) Seawater chemistry and early carbonate biomineralization. *Science* 316(5829):1302.
16. Kobayashi I (1980) *Various Patterns in Biomineralization and Its Phylogenetic Significances in Bivalve Molluscs*, eds Omori M, Watabe SW (Tokai Univ Press, Tokyo, Japan), pp 145–155.
17. Carter JG (1990) *Skeletal Biomineralization: Patterns, Processes, and Evolutionary Trends* (Van Nostrand Reinhold, New York).
18. Saruwatari K, Matsui T, Mukai H, Nagasawa H, Kogure T (2009) Nucleation and growth of aragonite crystals at the growth front of nacre in pearl oyster, *Pinctada fucata*. *Biomaterials* 30(16):3028–3034.
19. Plazzi F, Passamonti M (2010) Towards a molecular phylogeny of mollusks: Bivalves' early evolution as revealed by mitochondrial genes. *Mol Phylogenet Evol* 57(2): 641–657.
20. Cunha RL, Blanc F, Bonhomme F, Arnaud-Haond S (2011) Evolutionary patterns in pearl oysters of the genus *Pinctada* (Bivalvia: Pteriidae). *Mar Biotechnol (NY)* 13(2): 181–192.
21. Sudo S, et al. (1997) Structures of mollusc shell framework proteins. *Nature* 387(6633): 563–564.
22. Grégoire C (1972) *Structure of the Molluscan Shell*, eds Florin M, Scheer BT (Academic Press, New York), pp 45–102.
23. Wetzel G (1900) Die organischen Substanzen der Schalen von *Mytilus* und *Pinna* [The organic matter of *Mytilus* and *Pinna* shells]. *Z Phys Chem* 29:386–410.
24. Hare PE (1963) Amino acids in the proteins from aragonite and calcite in the shells of *Mytilus californianus*. *Science* 139(3551):216–217.
25. Weiner S (1983) Mollusk shell formation: Isolation of two organic matrix proteins associated with calcite deposition in the bivalve *Mytilus californianus*. *Biochemistry* 22:4139–4145.
26. Miyamoto H, et al. (1996) A carbonic anhydrase from the nacreous layer in oyster pearls. *Proc Natl Acad Sci USA* 93(18):9657–9660.
27. Miyashita T, Takagi R, Miyamoto H, Matsushiro A (2002) Identical carbonic anhydrase contributes to nacreous or prismatic layer formation in *Pinctada fucata* (Mollusca: Bivalvia). *Veliger* 45:250–255.
28. Marin F, Luquet G, Marie B, Medakovic D (2008) Molluscan shell proteins: Primary structure, origin, and evolution. *Curr Top Dev Biol* 80:209–276.
29. Marin F, Le Roy N, Silva P, Marie B (2012) The formation and mineralization of mollusk shell. *Front Biosci* 4:1099–1125.
30. Takeuchi T, Endo K (2006) Biphasic and dually coordinated expression of the genes encoding major shell matrix proteins in the pearl oyster *Pinctada fucata*. *Mar Biotechnol (NY)* 8(1):52–61.
31. Gardner LD, Mills D, Wiegand A, Leavesley D, Elizur A (2011) Spatial analysis of biomineralization associated gene expression from the mantle organ of the pearl oyster *Pinctada maxima*. *BMC Genomics* 12:455.
32. Jackson DJ, et al. (2006) A rapidly evolving secretome builds and patterns a sea shell. *BMC Biol* 4:40.
33. Nudelman F, Chen HH, Goldberg HA, Weiner S, Addadi L (2007) Spiers Memorial Lecture. Lessons from biomineralization: Comparing the growth strategies of mollusk shell prismatic and nacreous layers in *Atrina rigida*. *Faradays Discuss* 136:9–25.
34. Thompson JB, et al. (2000) Direct observation of the transition from calcite to aragonite growth as induced by abalone shell proteins. *Biophys J* 79(6):3307–3312.
35. Jackson DJ, et al. (2010) Parallel evolution of nacre building gene sets in molluscs. *Mol Biol Evol* 27(3):591–608.
36. Zentz F, et al. (2001) Characterization and quantification of chitosan extracted from nacre of the abalone *Haliotis tuberculata* and the oyster *Pinctada maxima*. *Mar Biotechnol (NY)* 3(1):36–44.
37. Suzuki M, Sakuda S, Nagasawa H (2007) Identification of chitin in the prismatic layer of the shell and a chitin synthase gene from the Japanese pearl oyster, *Pinctada fucata*. *Biosci Biotechnol Biochem* 71(7):1735–1744.
38. Bédouet L, et al. (2007) Heterogeneity of proteinase inhibitors in the water-soluble organic matrix from the oyster nacre. *Mar Biotechnol (NY)* 9(4):437–449.
39. Marie B, et al. (2010) Proteomic analysis of the organic matrix of the abalone *Haliotis asinina* calcified shell. *Proteome Sci* 8:54.
40. Taylor J, Kennedy WJ, Hall A (1973) The shell structure and mineralogy of the Bivalvia, Part II, *Lucinacea*. *Clavagellacea Bull Brit Mus Zool* 22:253–294.
41. Palmer AR (1992) Calcification in marine molluscs: How costly is it? *Proc Natl Acad Sci USA* 89(4):1379–1382.
42. Mao Che L, Golubic S, Le Campion-Alsumard T, Payri C (2001) Developmental aspects of biomineralization in the Polynesian pearl oyster *Pinctada margaritifera* var. *cumingii*. *Oceanol Acta* 24:537–549.
43. Yokoo N, et al. (2011) Microstructures of the larval shell of a pearl oyster, *Pinctada fucata*, investigated by FIB-TEM technique. *Am Mineral* 96:1020–1027.
44. Weiss IM, Tuross N, Addadi L, Weiner S (2002) Mollusk larval shell formation: Amorphous calcium carbonate is a precursor phase for aragonite. *J Exp Zool* 293(5):478–491.
45. Runnegar B (1983) Molluscan phylogeny revisited. *Mem Ass Australas Paleontols* 1: 121–144.
46. Carter JG, Clark GR II (1985) *Classification and Phylogenetic Significance of Mollusk Shell Microstructures*, ed Broadhead TW (Univ of Tennessee Press, Knoxville, TN), pp 50–71.
47. Farre B, et al. (2011) Shell layers of the black-lip pearl oyster *Pinctada margaritifera*: Matching microstructure and composition. *Comp Biochem Physiol B Biochem Mol Biol* 159(3):131–139.
48. Saleuddin ASM, Petit H (1983) *The Mollusca* (Academic Press, New York), Vol 4, pp 299–234.
49. Rousseau M, et al. (2009) Dynamics of sheet nacre formation in bivalves. *J Struct Biol* 165(3):190–195.
50. Joubert C, et al. (2010) Transcriptome and proteome analysis of *Pinctada margaritifera* calcifying mantle and shell: Focus on biomineralization. *BMC Genomics* 11:613.
51. Fang Z, Feng Q, Chi Y, Xie L, Zhang R (2008) Investigation of cell proliferation and differentiation in the mantle of *Pinctada fucata* (Bivalve, Mollusca). *Mar Biol* 153: 745–754.
52. Fleury C, et al. (2008) Shell repair process in the green ormer *Haliotis tuberculata*: A histological and microstructural study. *Tissue Cell* 40(3):207–218.
53. Cuif J-P, et al. (2011) Is the pearl layer a reverse shell? A re-examination of the theory of the pearl formation through physical characterizations of pearl and shell development stages in *Pinctada margaritifera*. *Aquat Liv Res* 24:411–424.
54. Weiner S, Addadi L (2012) Crystallization pathways in biomineralization. *Annu Rev Mater Res* 41:21–40.